

Scalable Gaussian Process Classification via Expectation Propagation

Daniel Hernández-Lobato
 Universidad Autónoma de Madrid
 Francisco Tomás y Valiente 11
 28049, Madrid, Spain
 daniel.hernandez@uam.com

José Miguel Hernández-Lobato
 Harvard University
 33 Oxford street
 Cambridge, MA 02138, USA
 jmhl@seas.harvard.edu

Abstract

Variational methods have been recently considered for scaling the training process of Gaussian process classifiers to large datasets. As an alternative, we describe here how to train these classifiers efficiently using expectation propagation. The proposed method allows for handling datasets with millions of data instances. More precisely, it can be used for (i) training in a distributed fashion where the data instances are sent to different nodes in which the required computations are carried out, and for (ii) maximizing an estimate of the marginal likelihood using a stochastic approximation of the gradient. Several experiments indicate that the method described is competitive with the variational approach.

1 Introduction

Gaussian process classification is a popular framework that can be used to address supervised machine learning problems in which the task of interest is to predict the class label associated to a new instance given some observed data [1]. In the binary classification case, this task is typically modeled by considering a non-linear latent function f whose sign at each input location determines the corresponding class label. A practical difficulty is, however, that making inference about f in this setting is infeasible due to the non-Gaussianity of the likelihood. Nevertheless, very efficient methods can be used to carry out the required computations in an approximate way [2, 3]. The result is a non-parametric classifier that becomes more expressive as the number of training instances increases. Unfortunately, the cost of all these methods is $\mathcal{O}(n^3)$, where n is the number of instances.

The computational cost described can be improved by using a sparse representation for the Gaussian process f [4]. A popular approach in this setting introduces additional data in the form of $m \ll n$ inducing points, whose location is inferred during the training process by maximizing some function [5, 6]. This leads to a reduced training cost that scales like $\mathcal{O}(nm^2)$. A limitation is, however, that the function to be maximized cannot be expressed as a sum over the data instances. This prevents using efficient techniques for maximization, such as stochastic gradient ascent or distributed computations. An exception is the work described in [7], which combines ideas from stochastic variational inference [8] and from variational Gaussian processes [9] to provide a scalable method for Gaussian process classification that can be applied to datasets with millions of data instances.

We introduce here an alternative to the variational approach described in [7] that is based on expectation propagation (EP) [10]. In particular, we show that in EP it is possible to compute a posterior approximation for the Gaussian process f and to update the model hyper-parameters, including the inducing points, at the same time. Moreover, in our EP formulation the marginal likelihood estimate is expressed as a sum over the data. This enables using stochastic methods to maximize such an estimate to find the model hyper-parameters. The EP updates can also be implemented in a distributed fashion, by spiting the data across several computational nodes. Summing up, our EP formulation has the same advantages as the variational approach from [7], with the convenience that all computations are tractable and univariate quadrature methods are not required, which is not the case of [7]. Finally, several experiments, involving

datasets with several millions of instances, show that both approaches for Gaussian process classification perform similarly in terms of prediction performance.

2 Scalable Gaussian process classification

We briefly introduce Gaussian process classification and the model we use. Then, we show how expectation propagation (EP) can be used for training in a distributed fashion and how the model hyper-parameters can be inferred using a stochastic approximation of the gradient of the estimate of the marginal likelihood. See the supplementary material for full details on the proposed EP method.

2.1 Gaussian process classification and sparse representations

Assume some observed data in the form of a matrix of attributes $\mathbf{X} = (\mathbf{x}_1, \dots, \mathbf{x}_n)^T$ with associated labels $\mathbf{y} = (y_1, \dots, y_n)$, where $y_i \in \{-1, 1\}$. The task is to predict the class label of a new instance. For this, it is assumed the labeling rule $y_i = \text{sign}(f(\mathbf{x}_i) + \epsilon_i)$, where $f(\cdot)$ is a non-linear function and ϵ_i is standard Gaussian noise with probability density $\mathcal{N}(\epsilon_i|0, 1)$. Furthermore, we assume a Gaussian process prior over f with zero mean and some covariance function $k(\cdot, \cdot)$ [1]. That is, $f \sim \mathcal{GP}(0, k(\cdot, \cdot))$. To make inference about $\mathbf{f} = (f(\mathbf{x}_1), \dots, f(\mathbf{x}_n))^T$ given the observed labels \mathbf{y} , Bayes' rule can be used. Namely, $p(\mathbf{f}|\mathbf{y}) = p(\mathbf{y}|\mathbf{f})p(\mathbf{f})/p(\mathbf{y})$ where $p(\mathbf{f})$ is a multivariate Gaussian distribution and $p(\mathbf{y})$ can be maximized to find the parameters of the covariance function k . The likelihood of \mathbf{f} is $p(\mathbf{y}|\mathbf{f}) = \prod_{i=1}^n \Phi(y_i f_i)$, where $\Phi(\cdot)$ is the cdf of a standard Gaussian and $f_i = f(\mathbf{x}_i)$. This is a non-Gaussian likelihood which makes the posterior intractable. However, there are techniques such as the Laplace approximation, expectation propagation or variational inference, that can be used to get a Gaussian approximation of $p(\mathbf{f}|\mathbf{y})$ [2, 3]. They all result in a non-parametric classifier. Unfortunately, these methods scale like $\mathcal{O}(n^3)$, where n is the number of instances.

Using a sparse representation for the Gaussian process f reduces the training cost. A popular method introduces a dataset of $m \ll n$ inducing points $\bar{\mathbf{X}} = (\bar{\mathbf{x}}_1, \dots, \bar{\mathbf{x}}_m)^T$ with associated values $\bar{\mathbf{f}} = (f(\bar{\mathbf{x}}_1), \dots, f(\bar{\mathbf{x}}_m))^T$ [6, 5]. The prior for f is then approximated as $p(\mathbf{f}) = \int p(\mathbf{f}|\bar{\mathbf{f}})p(\bar{\mathbf{f}}|\bar{\mathbf{X}})d\bar{\mathbf{f}} \approx \int [\prod_{i=1}^n p(f_i|\bar{\mathbf{f}})] p(\bar{\mathbf{f}}|\bar{\mathbf{X}})d\bar{\mathbf{f}} = p_{\text{FITC}}(\mathbf{f}|\bar{\mathbf{X}})$, where the Gaussian conditional $p(\mathbf{f}|\bar{\mathbf{f}})$ has been replaced by a factorized distribution $\prod_{i=1}^n p(f_i|\bar{\mathbf{f}})$. This approximation is known as the full independent training conditional (FITC) [4], and it leads to a prior $p_{\text{FITC}}(\mathbf{f}|\bar{\mathbf{X}})$ with a low-rank covariance matrix. This prior allows for approximate inference with a cost linear in n , *i.e.*, $\mathcal{O}(nm^2)$. Finally, the inducing points $\bar{\mathbf{X}}$ can be seen as prior hyper-parameters to be learnt by maximizing $p(\mathbf{y})$.

2.2 Model specification and expectation propagation algorithm

The first methods based on the FITC approximation do not express the estimate of $p(\mathbf{y})$ as a sum across data instances [6, 5]. This makes difficult the use of efficient algorithms for learning the model hyper-parameters. To avoid this, we follow [9] and do not marginalize the values $\bar{\mathbf{f}}$ associated to the inducing points. Specifically, the posterior approximation is $p(\mathbf{f}|\mathbf{y}) \approx \int p(\mathbf{f}|\bar{\mathbf{f}})q(\bar{\mathbf{f}})d\bar{\mathbf{f}}$, where q is a Gaussian distribution that approximates $p(\bar{\mathbf{f}}|\mathbf{y})$, *i.e.*, the posterior of the values associated to the inducing points. To obtain q we use first the FITC approximation on the exact posterior:

$$p(\bar{\mathbf{f}}|\mathbf{y}) = \frac{\int p(\mathbf{y}|\mathbf{f})p(\mathbf{f}|\bar{\mathbf{f}})d\mathbf{f}p(\bar{\mathbf{f}}|\bar{\mathbf{X}})}{p(\mathbf{y}|\bar{\mathbf{X}})} \approx \frac{\int p(\mathbf{y}|\mathbf{f})p_{\text{FITC}}(\mathbf{f}|\bar{\mathbf{f}})d\mathbf{f}p(\bar{\mathbf{f}}|\bar{\mathbf{X}})}{p(\mathbf{y}|\bar{\mathbf{X}})} = \frac{\prod_{i=1}^n \phi_i(\bar{\mathbf{f}})p(\bar{\mathbf{f}}|\bar{\mathbf{X}})}{p(\mathbf{y}|\bar{\mathbf{X}})}, \quad (1)$$

where $p(\mathbf{y}|\mathbf{f}) = \prod_{i=1}^n \Phi(y_i f_i)$, $p_{\text{FITC}}(\mathbf{f}|\bar{\mathbf{f}}) = \prod_{i=1}^n p(f_i|\bar{\mathbf{f}}) = \prod_{i=1}^n \mathcal{N}(f_i|m_i, s_i)$ and $\phi_i(\bar{\mathbf{f}}) = \int \Phi(y_i f_i) \mathcal{N}(f_i|m_i, s_i)df_i = \Phi(y_i m_i/\sqrt{s_i + 1})$, with $m_i = \mathbf{K}_{f_i \bar{\mathbf{f}}} \mathbf{K}_{\bar{\mathbf{f}} \bar{\mathbf{f}}}^{-1} \bar{\mathbf{f}}$ and $s_i = \mathbf{K}_{f_i f_i} - \mathbf{K}_{f_i \bar{\mathbf{f}}} \mathbf{K}_{\bar{\mathbf{f}} \bar{\mathbf{f}}}^{-1} \mathbf{K}_{\bar{\mathbf{f}} f_i}$. Moreover, $\mathbf{K}_{\bar{\mathbf{f}} \bar{\mathbf{f}}}$ is a matrix with the prior covariances among the entries in $\bar{\mathbf{f}}$, $\mathbf{K}_{f_i \bar{\mathbf{f}}}$ is a row vector with the prior covariances between f_i and $\bar{\mathbf{f}}$ and $\mathbf{K}_{f_i f_i}$ is the prior variance of f_i .

The r.h.s. of (1) is an intractable posterior due to the non-Gaussianity of each ϕ_i . We use expectation propagation (EP) to obtain a Gaussian approximation q [10]. In EP each ϕ_i is approximated as:

$$\phi_i(\bar{\mathbf{f}}) = \Phi\left(\frac{y_i m_i}{\sqrt{s_i + 1}}\right) \approx \tilde{\phi}_i(\bar{\mathbf{f}}) = \tilde{s}_i \exp\left\{-\frac{\tilde{\nu}_i \bar{\mathbf{f}}^T \mathbf{v}_i \mathbf{v}_i^T \bar{\mathbf{f}} + \tilde{\mu}_i \bar{\mathbf{f}}^T \mathbf{v}_i}{2}\right\}, \quad (2)$$

where $\tilde{\phi}_i$ is an un-normalized Gaussian factor, $\mathbf{v}_i = \mathbf{K}_{\bar{\mathbf{f}}\bar{\mathbf{f}}}^{-1} \mathbf{K}_{\bar{\mathbf{f}}f_i}$ is a m dimensional vector, and \tilde{s}_i , $\tilde{\nu}_i$ and $\tilde{\mu}_i$ are parameters to be estimated by EP. Importantly, $\tilde{\phi}_i$ has a one-rank precision matrix, which means that in practice only $\mathcal{O}(m)$ parameters need to be stored per each $\tilde{\phi}_i$. This is not an approximation and the optimal approximate factor $\tilde{\phi}_i$ has this form (see the supplementary material). The posterior approximation q is obtained by replacing in the r.h.s. of (1) each exact factor ϕ_i with the corresponding approximate factor $\tilde{\phi}_i$. Namely, $q(\bar{\mathbf{f}}) = \prod_{i=1}^n \tilde{\phi}_i(\bar{\mathbf{f}}) p(\bar{\mathbf{f}}|\bar{\mathbf{X}}) / Z_q$, where Z_q is a normalization constant that approximates the marginal likelihood $p(\mathbf{y}|\bar{\mathbf{X}})$. All factors in q are Gaussian, including the prior. Thus, q is a multivariate Gaussian distribution over m dimensions.

EP updates each $\tilde{\phi}_i$ iteratively until-convergence as follows. First, $\tilde{\phi}_i$ is removed from q by computing $q^{\setminus i} \propto q / \tilde{\phi}_i$. Then, we minimize the Kullback-Leibler divergence between $Z_i^{-1} \phi_i q^{\setminus i}$, and q , *i.e.*, $\text{KL}[Z_i^{-1} \phi_i q^{\setminus i} || q]$, with respect to q , where Z_i is the normalization constant of $\phi_i q^{\setminus i}$. This can be done by matching the mean and the covariances of $Z_i^{-1} \phi_i q^{\setminus i}$, which can be obtained from the derivatives of $\log Z_i$ with respect to the (natural) parameters of $q^{\setminus i}$. Given an updated distribution q , the approximate factor is $\tilde{\phi}_i = Z_i q / q^{\setminus i}$. This guarantees that $\tilde{\phi}_i$ is similar to ϕ_i in regions of high posterior probability as estimated by $q^{\setminus i}$ [11]. These updates are done in parallel for efficiency reasons, *i.e.*, we compute $q^{\setminus i}$ and the new q , for $i = 1 \dots n$, at the same time, and then update $\tilde{\phi}_i$ as before [12]. The new approximation q is obtained by multiplying all the $\tilde{\phi}_i$ and $p(\bar{\mathbf{f}}|\bar{\mathbf{X}})$. The normalization constant of q , Z_q , is the EP approximation of $p(\mathbf{y}|\bar{\mathbf{X}})$. The log of this constant is

$$\log Z_q = g(\boldsymbol{\theta}) - g(\boldsymbol{\theta}_{\text{prior}}) + \sum_{i=1}^n \log \tilde{Z}_i \quad \log \tilde{Z}_i = \log Z_i + g(\boldsymbol{\theta}^{\setminus i}) - g(\boldsymbol{\theta}), \quad (3)$$

where $\boldsymbol{\theta}$, $\boldsymbol{\theta}^{\setminus i}$ and $\boldsymbol{\theta}_{\text{prior}}$ are the natural parameters of q , $q^{\setminus i}$ and $p(\bar{\mathbf{f}}|\bar{\mathbf{X}})$, respectively; and $g(\boldsymbol{\theta})$ is the log-normalizer of a multivariate Gaussian with natural parameters $\boldsymbol{\theta}$. See [13] for further details.

At convergence, the gradient of $\log Z_q$ with respect to the parameters of any $\tilde{\phi}_i$ is zero [13]. Thus, it is possible to evaluate the gradient of $\log Z_q$ with respect to a hyper-parameter ξ_j (*i.e.*, a parameter of the covariance function k or a component of $\bar{\mathbf{X}}$) (see the supplementary material). In particular,

$$\frac{\partial \log Z_q}{\partial \xi_j} = \boldsymbol{\eta}^T \frac{\partial \boldsymbol{\theta}_{\text{prior}}}{\partial \xi_j} - \boldsymbol{\eta}_{\text{prior}}^T \frac{\partial \boldsymbol{\theta}_{\text{prior}}}{\partial \xi_j} + \sum_{i=1}^n \frac{\partial \log Z_i}{\partial \xi_j}, \quad (4)$$

where $\boldsymbol{\eta}$ and $\boldsymbol{\eta}_{\text{prior}}$ are the expected sufficient statistics under q and the prior $p(\bar{\mathbf{f}}|\bar{\mathbf{X}})$, respectively. With these gradients we can easily estimate all the model hyper-parameters by maximizing $\log Z_q$. Moreover, it is also possible to use q to estimate the distribution of the label y_* of a new instance \mathbf{x}_* :

$$p(y_*|\mathbf{y}, \bar{\mathbf{X}}) \approx \int p(y_*|f_*) p(f_*|\bar{\mathbf{f}}) q(\bar{\mathbf{f}}) d\bar{\mathbf{f}} df_*. \quad (5)$$

Last, because several simplifications occur when computing the derivatives with respect to the inducing points [14], the running time of EP, including hyper-parameter optimization, is $\mathcal{O}(nm^2)$.

2.3 Scalable expectation propagation

A drawback of EP is that the hyper-parameters of the model are updated via gradient ascent only after convergence, which is when (4) is valid. This is very inefficient at the initial iterations, in which the estimates of the model hyper-parameters are very poor, and EP may require several iterations to converge. We propose to update the approximate factors $\tilde{\phi}_i$ and the model hyper-parameters ξ_j at the same time. That is, after a parallel update of all the approximate factors, we update the hyper-parameters using gradient

ascent assuming that each $\tilde{\phi}_i$ is fixed. Because EP has not converged, the moments of $Z_i^{-1}\phi_i q^{\setminus i}$ and q need not match. Thus, extra terms must be added in (4) to get the gradient. Nevertheless, our experiments show that the extra terms are very small and can be ignored. In practice, we use (4) for the inner update of the hyper-parameters. Figure 1 (left) shows that this approach successfully maximizes $\log Z_q$ on the *Pima* dataset from the UCI repository [15]. Because we do not wait for convergence in EP, the method is significantly faster. The idea of why this works is as follows. The EP update of each $\tilde{\phi}_i$ can be seen as a (natural) gradient descent step on $\log Z_q$ when $\tilde{\phi}_j$, with $j \neq i$, remain fixed [16]. Furthermore, those updates are very effective for finding a stationary point of $\log Z_q$ (see [10] for further details). Thus, it is natural that an inner update of the hyper-parameters when all $\tilde{\phi}_i$ remain fixed is an effective method for finding a maximum of $\log Z_q$.

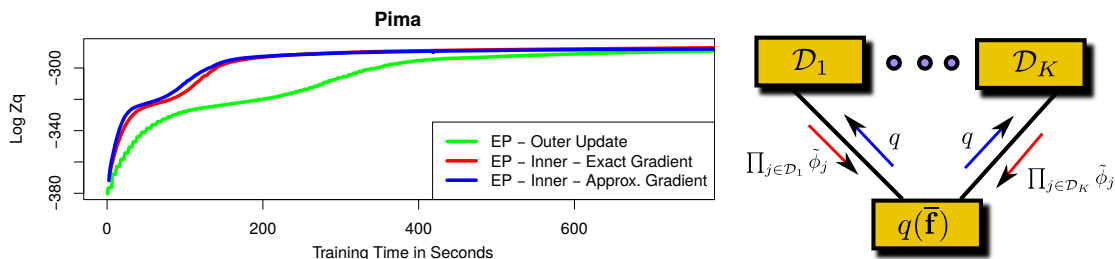


Figure 1: (left) Value of $\log Z_q$ obtained when updating the hyper-parameters after EP has converged (outer) and just after each update of the approximate factors $\tilde{\phi}_i$ (inner), when using the exact gradient, and the approximation (4), which assumes matched moments between $Z_i^{-1}\phi_i q^{\setminus i}$ and q . $m = 300$. (right) Distribution of the EP updates across K computational nodes storing a subset $\mathcal{D}_1, \dots, \mathcal{D}_K$ of the data. Best seen in color.

Distributed training: The method described is suitable for distributed computation using the ideas in [17]. In particular, the training data can be split in K subsets $\mathcal{D}_1, \dots, \mathcal{D}_K$ which are sent to K computational nodes. A master node stores the posterior approximation q , which is sent to each computational node. Then, node k updates each $\tilde{\phi}_j$ with $j \in \mathcal{D}_k$ and returns $\prod_{j \in \mathcal{D}_k} \tilde{\phi}_j$ to the master node. After each node has done this, the master node updates q using $p(\bar{\mathbf{f}}|\bar{\mathbf{X}})$ and the messages received. Because the gradient of the hyper-parameters (4) involves a sum over the data instances, its computation can also be distributed among the K computational nodes. Thus, the training cost of the EP method can be reduced to $\mathcal{O}(n/Km^2)$. Figure (1) (right) illustrates the scheme described.

Training using minibatches: The method described is also suitable for stochastic optimization. In this case the data are split in minibatches \mathcal{M}_k of size at most m , the number of inducing points. For each minibatch \mathcal{M}_k , each $\tilde{\phi}_j$ with $j \in \mathcal{M}_k$ is refined, and q is updated afterwards. Next, the model hyper-parameters are updated via gradient ascent using a stochastic approximation of (4). Namely,

$$\frac{\partial Z_q}{\partial \xi_j} \approx \boldsymbol{\eta}^\top \frac{\partial \boldsymbol{\theta}_{\text{prior}}}{\partial \xi_j} - \boldsymbol{\eta}_{\text{prior}}^\top \frac{\partial \boldsymbol{\theta}_{\text{prior}}}{\partial \xi_j} + \frac{n}{|\mathcal{M}_k|} \sum_{l \in \mathcal{M}_k} \frac{\partial \log Z_l}{\partial \xi_j}. \quad (6)$$

After the update, q is reconstructed. With this training scheme we allow for more frequent updates of the model hyper-parameters and the training cost scales like $\mathcal{O}(m^3)$. The memory requirements scale, however, like $\mathcal{O}(nm)$, since we need to store the parameters of each approximate factor ϕ_i .

3 Related work

A related method for binary classification with GPs uses scalable variational inference (SVI) [7]. Since $p(\mathbf{y}|\bar{\mathbf{f}}) = \int p(\mathbf{y}|\mathbf{f})p(\bar{\mathbf{f}}|\bar{\mathbf{f}})d\bar{\mathbf{f}}$, we obtain the bound $\log p(\mathbf{y}|\bar{\mathbf{f}}) \geq \mathbb{E}_{p(\bar{\mathbf{f}}|\bar{\mathbf{f}})}[\log p(\mathbf{y}|\bar{\mathbf{f}})]$ by taking the logarithm and using Jensen's inequality. Let $q(\bar{\mathbf{f}})$ be a Gaussian approximation of $p(\bar{\mathbf{f}}|\bar{\mathbf{f}})$. Then,

$$\log p(\mathbf{y}) = \log \int q(\bar{\mathbf{f}})p(\mathbf{y}|\bar{\mathbf{f}})p(\bar{\mathbf{f}}|\bar{\mathbf{X}})/q(\bar{\mathbf{f}})d\bar{\mathbf{f}} \geq \mathbb{E}_{q(\bar{\mathbf{f}})}[\log p(\mathbf{y}|\bar{\mathbf{f}})] - \text{KL}[q(\bar{\mathbf{f}})||p(\bar{\mathbf{f}}|\bar{\mathbf{X}})], \quad (7)$$

by Jensen’s inequality, with $\text{KL}[\cdot|\cdot]$ a Kullback Leibler divergence. Using the first bound in (7) gives

$$\begin{aligned} \log p(\mathbf{y}) &\geq \mathbb{E}_{q(\bar{\mathbf{f}})}[\mathbb{E}_{p(\mathbf{f}|\bar{\mathbf{f}})}[\log p(\mathbf{y}|\mathbf{f})]] - \text{KL}[q(\bar{\mathbf{f}})||p(\bar{\mathbf{f}}|\bar{\mathbf{X}})] \geq \mathbb{E}_{q(\mathbf{f})}[\log p(\mathbf{y}|\mathbf{f})] - \text{KL}[q(\bar{\mathbf{f}})||p(\bar{\mathbf{f}}|\bar{\mathbf{X}})] \\ &\geq \sum_{i=1}^n \mathbb{E}_{q(f_i)}[\log p(y_i|f_i)] - \text{KL}[q(\bar{\mathbf{f}})||p(\bar{\mathbf{f}}|\bar{\mathbf{X}})], \end{aligned} \quad (8)$$

where $q(\mathbf{f}) = \int p(\mathbf{f}|\bar{\mathbf{f}})q(\bar{\mathbf{f}})d\bar{\mathbf{f}}$ and $q(f_i)$ is the i -th marginal of $q(\mathbf{f})$. Let $q(\bar{\mathbf{f}}) = \mathcal{N}(\bar{\mathbf{u}}|\mathbf{m}, \mathbf{S})$, with \mathbf{m} and \mathbf{S} variational parameters. Because $p(\mathbf{f}|\bar{\mathbf{f}}) = \mathcal{N}(\mathbf{f}|\mathbf{A}\bar{\mathbf{f}}, \mathbf{K}_{\mathbf{ff}} - \mathbf{A}\mathbf{K}_{\bar{\mathbf{f}\bar{\mathbf{f}}}}^{-1})$, where $\mathbf{A} = \mathbf{K}_{\bar{\mathbf{f}\bar{\mathbf{f}}}}^{-1}$, and $\mathbf{K}_{\bar{\mathbf{f}\bar{\mathbf{f}}}}$ is a matrix with the covariances between pairs of observed inputs and inducing points,

$$q(\mathbf{f}) = \mathcal{N}(\mathbf{f}|\mathbf{A}\mathbf{m}, \mathbf{K}_{\mathbf{ff}} + \mathbf{A}(\mathbf{S} - \mathbf{K}_{\bar{\mathbf{f}\bar{\mathbf{f}}}})\mathbf{A}^T). \quad (9)$$

\mathbf{S} is encoded in practice as $\mathbf{L}\mathbf{L}^T$ and the lower bound (8) is maximized with respect to \mathbf{m} , \mathbf{L} , the inducing points $\bar{\mathbf{X}}$ and any hyper-parameter in the covariance function using either batch, stochastic or distributed optimization techniques. In the stochastic case, small minibatches are considered and the gradient of $\sum_{i=1}^n \mathbb{E}_{q(f_i)}[\log p(y_i|f_i)]$ in (8) is subsampled and scaled accordingly to obtain an estimate of the exact gradient. In the distributed case, the gradient of the sum is computed in parallel. Once (8) has been optimized, (5) can be used for making predictions. The computational cost of this method is $\mathcal{O}(nm^2)$, when trained in a batch setting, and $\mathcal{O}(m^3)$, when using minibatches and stochastic gradients. A practical disadvantage is, however, that $\mathbb{E}_{q(f_i)}[\log p(y_i|f_i)]$ has no analytic solution. Importantly, these expectations and their gradients must be approximated using quadrature techniques. By contrast, in the proposed EP method all computations have a closed-form solution.

In the generalized FITC approximation (GFITC) [6] the values $\bar{\mathbf{f}}$ associated to the inducing points are marginalized, as indicated in Section 2.1. This generates the FITC prior $p_{\text{FITC}}(\mathbf{f}|\bar{\mathbf{X}})$ which leads to a computational cost that is $\mathcal{O}(nm^2)$. Expectation propagation (EP) is also used in such a model to approximate $p(\mathbf{f}|\mathbf{y}, \bar{\mathbf{X}})$. In particular, EP replaces with a Gaussian factor each likelihood factor of the form $p(y_i|f_i) = \Phi(y_i|f_i)$. A limitation is, however, that the estimate of $p(\mathbf{y}|\bar{\mathbf{X}})$ provided by EP in this model does not contain a sum over the data instances. Thus, GFITC does not allow for stochastic nor distributed optimization of the model hyper-parameters, unlike the proposed approach.

A similar model to one described in Section 2.2 is found in [18]. There, EP is also used for approximate inference. However, the moments of the process are matched at \mathbf{f} , instead of at $\bar{\mathbf{f}}$. This leads to equivalent, but more complicated EP updates. Moreover, the inducing points (which are noisy) are not learned from the observed data, but kept fixed. This is a serious limitation. The main advantage with respect to GFITC is that training can be done in an online fashion, as in our proposed approach.

4 Experiments

We follow [7] and compare in several experiments the proposed method for Gaussian process classification based on a scalable EP algorithm (SEP) with (i) the generalized FITC approximation (GFITC) [6] and (ii) the scalable variational inference (SVI) method from [7]. SEP and GFITC use faster parallel EP updates that require only matrix multiplications and avoid loops over the data instances [12]. All methods are implemented in R. The code is found in the supplementary material.

4.1 Performance on datasets from the UCI repository

A first set of experiments evaluates the predictive performance of SEP, GFITC and SVI on 7 datasets extracted from the UCI repository [15]. We use 90% of the data for training and 10% for testing and report averages over 20 repetitions of the experiments. All methods are trained using batch algorithms for 250 iterations. Both GFITC and SVI use L-BFGS-B. We report for each method the average negative test log-likelihood. A squared exponential covariance function with automatic relevance determination, an amplitude parameter and an additive noise parameter is employed. The initial inducing points are chosen at random from the training data, but are the same for each method. All other hyper-parameters are initialized to the same values. A different number of inducing points m are considered. Namely, 15%, 25% and 50% of the total number of instances. The results of these experiments are displayed in Table 1. The best

performing method is highlighted in bold face. We observe that the proposed approach, *i.e.*, SEP, obtains similar results to GFITC and SVI and sometimes is the best performing method. Table 1 also reports the average training time of each method in seconds. The fastest method is SEP followed by SVI. GFITC is the slowest method since it runs EP until convergence to evaluate then the gradient of the approximate marginal likelihood. By contrast, SEP updates at the same time the approximate factors and the model hyper-parameters.

Table 1: Average negative test log likelihood for each method and average training time in seconds.

Problem	$m = 15\%$			$m = 25\%$			$m = 50\%$		
	GFITC	SEP	SVI	GFITC	SEP	SVI	GFITC	SEP	SVI
Australian	.68 ± .06	.69 ± .07	.63 ± .05	.68 ± .08	.67 ± .07	.63 ± .05	.67 ± .09	.64 ± .05	.63 ± .05
Breast	.10 ± .05	.11 ± .05	.10 ± .05	.11 ± .06	.11 ± .05	.10 ± .05	.11 ± .05	.11 ± .05	.10 ± .05
Crabs	.07 ± .07	.06 ± .06	.07 ± .06	.06 ± .07	.06 ± .06	.07 ± .07	.06 ± .07	.06 ± .06	.09 ± .06
Heart	.43 ± .12	.40 ± .13	.39 ± .11	.42 ± .12	.41 ± .12	.40 ± .11	.42 ± .13	.41 ± .11	.40 ± .10
Ionosphere	.30 ± .22	.26 ± .19	.26 ± .14	.29 ± .23	.27 ± .20	.27 ± .18	.30 ± .24	.27 ± .19	.26 ± .16
Pima	.54 ± .08	.52 ± .07	.49 ± .05	.53 ± .07	.51 ± .06	.50 ± .05	.53 ± .07	.50 ± .05	.49 ± .05
Sonar	.35 ± .13	.33 ± .10	.40 ± .17	.35 ± .12	.32 ± .10	.40 ± .19	.35 ± .13	.29 ± .09	.35 ± .16
Avg. Time	59 ± 4	17 ± 1	40 ± 2	133 ± 6	37 ± 2	65 ± 3	494 ± 29	130 ± 5	195 ± 10

4.2 Learning the location of the inducing points

Using the setting of the previous section, we focus on the two dimensional *Banana* dataset and analyze the location of the inducing points inferred by each method. We initialize the inducing points at random from the training set and progressively increase their number m from 4 to 128. Figure 2 shows the results obtained. For small values of m , *i.e.*, $m = 4$ or $m = 8$, SEP and SVI provide very similar locations for the inducing points. The estimates provided by GFITC for $m = 4$ are different as a consequence of arriving to a sub-optimal local maximum of the estimate of the marginal likelihood. If the initial inducing points are chosen differently, GFITC gives the same solution as SEP and SVI. We also observe that SEP and SVI quickly provide (*i.e.*, for $m = 16$) estimates of the decision boundaries that look similar to the ones obtained with larger values of m (*i.e.*, $m = 128$). These results confirm that SEP is able to find good locations for the inducing points. Finally, we note that SVI seems to prefer placing the inducing points near the decision boundaries. This is certainly not the case of GFITC nor SEP, which seems to inherit this behavior from GFITC.

4.3 Performance as a function of time

We profile each method and show the prediction performance on the *Image* datasets a function of the training time, for different numbers of inducing points $m = 4, 50, 200$. Again we use 90% of the data for training and 10% for testing. We report averages over 100 realizations of the experiments. The results obtained are displayed in Figure 3 (left). We observe that the proposed method SEP provides the best performance at the lowest computational time. It is faster than GFITC because in SEP we update the posterior approximation q and the hyper-parameters at the same time. By contrast, GFITC waits until EP has converged to update the hyper-parameters. SVI also takes more time than SEP to obtain a similar level of performance. This is because SVI requires a few extra matrix multiplications with cost $\mathcal{O}(nm^2)$ to evaluate the gradient of the hyper-parameters. Furthermore, the initial performance of SVI is worse than the one of GFITC and SEP. After one iteration, both GFITC and SEP have updated each approximate factor, leading to a good estimate of q , the posterior approximation, which is then used for hyper-parameter estimation. By contrast, SVI updates q using gradient descent which requires several iterations to get a good estimate of this distribution. Thus, at the beginning, SVI updates the model hyper-parameters when q is still a very bad approximation.

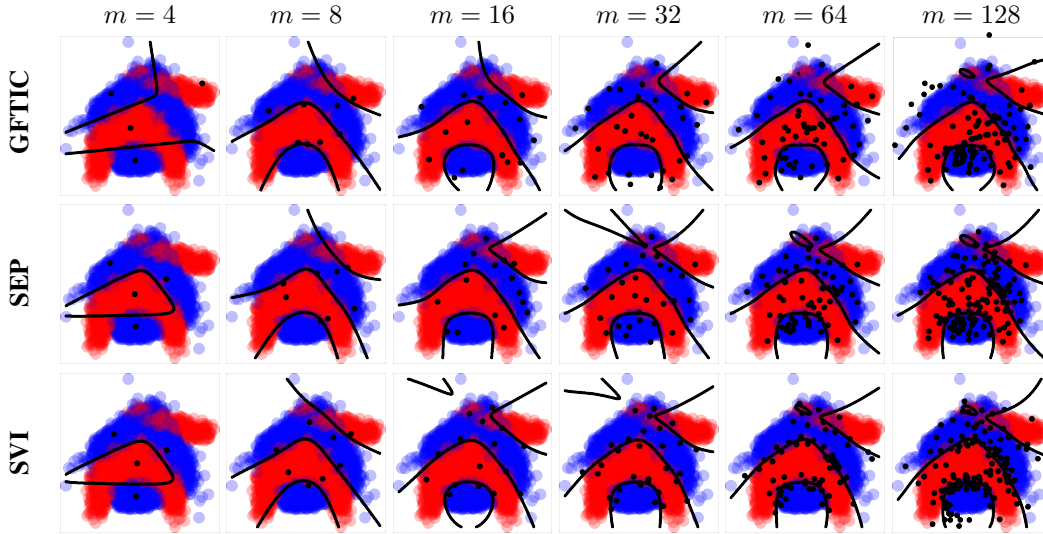


Figure 2: Effect of increasing the inducing points for SEP, SVI and GFITC. Each column shows a different number of inducing points from $m = 4$ to $m = 128$. Blue and red points represent training data from the banana dataset. Inducing points are black dots and decision boundaries are black lines. Best seen in color.

4.4 Training in a distributed fashion

We illustrate the utility of SEP and SVI to carry out distributed training (GFITC does not allow for this). We consider the MNIST dataset and use 60,000 instances for training and 10,000 instances for testing. The number of inducing points m is set equal to 200 in both SEP and SVI. The task is to discriminate odd from even digits, which is a highly non-linear problem. We distribute the data across an increasing number of nodes from 1 to 12 using a machine with 12 CPUs. The process of distributed training is simulated via the R package *doMC*, which allows to execute for loops in parallel with a few lines of code. In SVI we parallelize the computation of the terms (corresponding either to both the lower bound or the gradient) that depend on the training instances. In SEP we parallelize the updates of the approximate factors and the computation of the estimate of the gradient of hyper-parameters. Figure 3 (right) shows the training time in seconds of each method as a function of the number of nodes (CPUs) considered. We observe that using more than 1 nodes significantly reduces the training time of SEP and SVI, until 6 nodes are reached. After this, no improvements are observed, probably because process synchronization becomes a bottle-neck. The test error and the avg. neg. test log likelihood of SVI is 2.2% and 0.0655, respectively, while for SEP they are 2.7% and 0.0694. These values are the same independently of the number of nodes considered.

4.5 Training using minibatches and stochastic gradients

We evaluate the performance of SEP and SVI on the MNIST dataset considered before when the training process is implemented using minibatches of 200 instances. Each minibatch is used to update the posterior approximation q and to compute a stochastic approximation of the gradient of the hyper-parameters. Note that GFITC does not allow for this type of stochastic optimization. The learning rate employed for updating the hyper-parameters is computed using the Adadelta method in both SEP and SVI with $\rho = 0.9$ and $\epsilon = 10^{-5}$ [19]. The number of inducing points is set equal to the minibatch size, *i.e.*, 200. We report the performance on the test set (prediction error and average negative test log likelihood) as a function of the training time. We compare the results of these methods (stochastic) with the variants of SEP and SVI that use all data instances for the estimation of the gradient (batch). Figure 4 (top) shows the results obtained. We observe that stochastic methods (either SEP or SVI) obtain good results even before batch methods have completed a single hyper-parameter update. Furthermore, the performance of the stochastic variants of SEP and SVI in terms of the test error or the average negative log likelihood with respect to the running time is very similar.

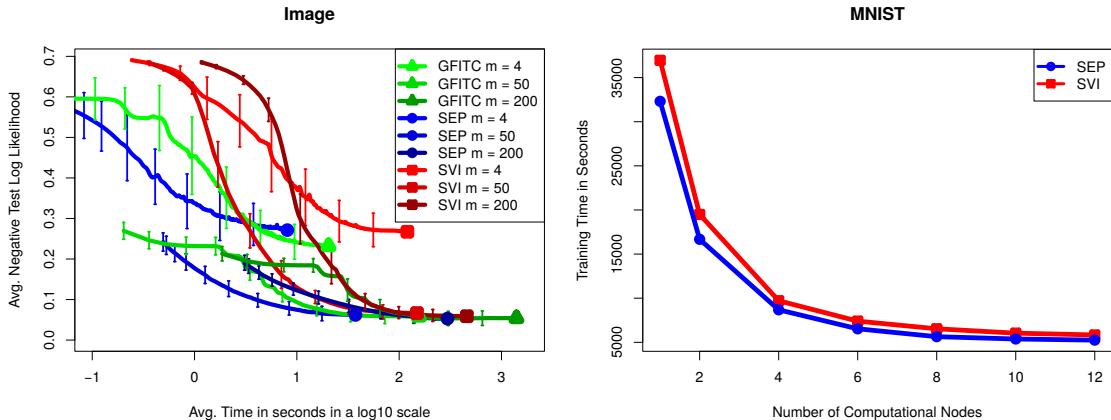


Figure 3: (left) Prediction performance of each method on the *Image* dataset as a function of the training time measured in seconds (in a \log_{10} scale). Different numbers of inducing points are considered, *i.e.*, $m = 4, 50, 200$. Best seen in color. (right) Average training time in seconds for SEP and SVI on the MNIST dataset as a function of the number of computational nodes employed in the process of distributed training.

Our last experiments consider information about all commercial flights in the USA from January 2008 to April 2008 (available at <http://stat-computing.org/dataexpo/2009/>). The task is the same as in [7]. Namely, to predict whether a flight was delayed or not based on 8 attributes: age of the aircraft, distance that needs to be covered, airtime, departure time, arrival time, day of the week, day of the month and month. After removing instances with missing values 2, 127, 068 instances remain. From these, 10, 000 are used for testing and the rest are used for training the stochastic variants of SVI and SEP (batch methods are infeasible in this dataset). We use a minibatch of size 200 and set $m = 200$ and compare results with a logistic regression classifier. The results obtained are displayed in Figure 4 (bottom). We observe that both SEP and SVI outperform the linear model, which shows that the problem is non-linear. Eventually SEP and SVI provide similar performance results, probably because in this large dataset the posterior distribution is very close to be Gaussian. However, SEP improves results more quickly. This supports that, at the beginning, the EP updates of SEP are more effective for estimating q than the gradient updates of SVI. More precisely, SVI is probably updating the hyper-parameters using a poor estimate of q during the first iterations.

5 Conclusions

We have shown that expectation propagation (EP) can be used for Gaussian process classification in large scale problems. Our scalable variant of EP (SEP) allows for (i) training in a distributed fashion in which the data are sent to different computational nodes and (ii) for updating the posterior approximation and the model hyper-parameters using minibatches and a stochastic approximation of the gradient of the estimate of the marginal likelihood. The proposed method, SEP, has been compared with other approaches from the literature such as the generalized FITC approximation (GFITC) and a scalable variational inference (SVI) method. Our results show that SEP outperforms GFITC in large datasets in which that method becomes infeasible. Furthermore, SEP is competitive with SVI and in large datasets provides the same or even better performance at a similar computational cost. If small minibatches are used for training, the computational cost of SEP is $\mathcal{O}(m^3)$, where m is the number of inducing points. A disadvantage is, however, that the memory requirements are $\mathcal{O}(nm)$, where n is the number of instances. Finally, SEP seems to provide better results than SVI at the beginning. This is probably due to a better estimation of the posterior approximation q by using the EP updates (free of any learning rate) than by the gradient steps employed by SVI.

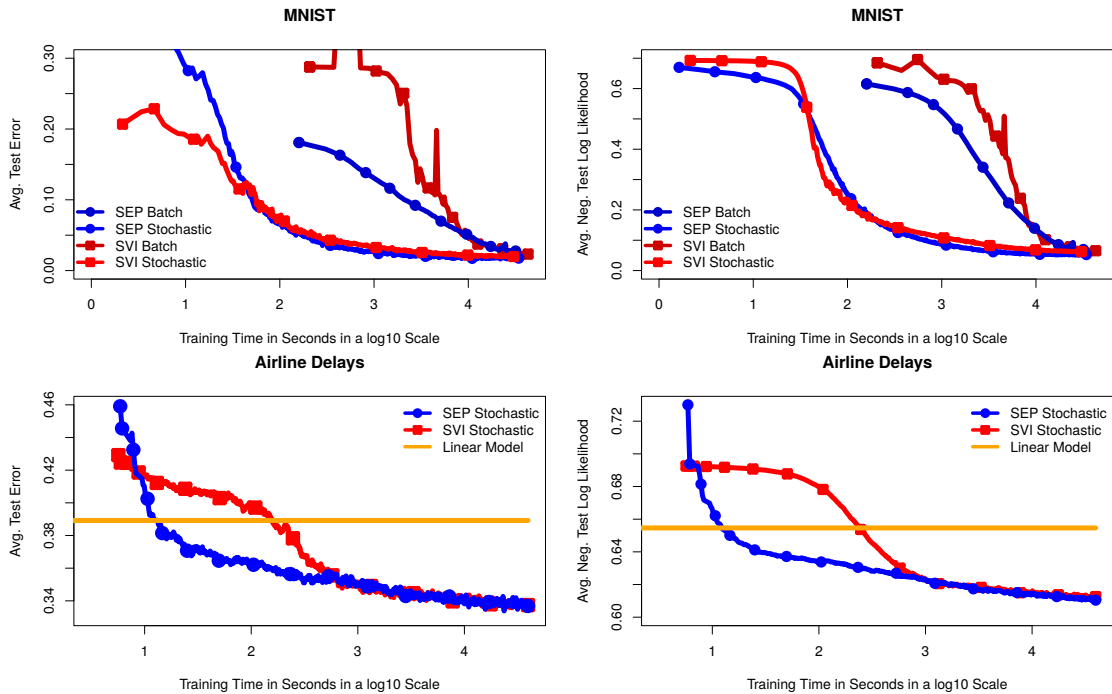


Figure 4: (top) Average test error and average negative test log likelihood for SEP and SVI as a function of training time on the MNIST dataset. We report results for the variants that use a minibatch size equal to 200 to approximate the gradients (stochastic) and for the variants that use all data instances for the gradient evaluation (batch). (bottom) Same results for the Airline delays dataset where batch methods are not feasible. The performance of a linear logistic regression classifier is also displayed. Best seen in color.

Acknowledgements

Daniel Hernández-Lobato gratefully acknowledges the use of the facilities of Centro de Computación Científica (CCC) at Universidad Autónoma de Madrid. This author also acknowledges financial support from Spanish Plan Nacional I+D+i, Grant TIN2013-42351-P, and from Comunidad de Madrid, Grant S2013/ICE-2845 CASI-CAM-CM. José Miguel Hernández-Lobato acknowledges financial support from the Rafael del Pino Foundation.

References

- [1] C.E. Rasmussen and C.K.I. Williams. *Gaussian Processes for Machine Learning*. The MIT Press, 2006.
- [2] M. Kuss and C.E. Rasmussen. Assessing approximate inference for binary Gaussian process classification. *Journal of Machine Learning Research*, 6:1679–1704, 2005.
- [3] H. Nickisch and C.E. Rasmussen. Approximations for binary Gaussian process classification. *Journal of Machine Learning Research*, 9:2035–2078, 2008.
- [4] J. Quiñero Candela and C.E. Rasmussen. A unifying view of sparse approximate Gaussian process regression. *Journal of Machine Learning Research*, pages 1935–1959, 2005.
- [5] E. Snelson and Z. Ghahramani. Sparse gaussian processes using pseudo-inputs. In *Advances in Neural Information Processing Systems 18*, 2006.
- [6] A. Naish-Guzman and S. Holden. The generalized FITC approximation. In *Advances in Neural Information Processing Systems 20*. 2008.

- [7] J. Hensman, A. Matthews, and Z. Ghahramani. Scalable variational Gaussian process classification. In *Proceedings of the Eighteenth International Conference on Artificial Intelligence and Statistics*, 2015.
- [8] M.D. Hoffman, D.M. Blei, C. Wang, and J. Paisley. Stochastic variational inference. *Journal of Machine Learning Research*, 14:1303–1347, 2013.
- [9] M. Titsias. Variational Learning of Inducing Variables in Sparse Gaussian Processes. In *International Conference on Artificial Intelligence and Statistics (AISTATS)*, 2009.
- [10] T. Minka. Expectation propagation for approximate Bayesian inference. In *Annual Conference on Uncertainty in Artificial Intelligence*, pages 362–36, 2001.
- [11] C. M. Bishop. *Pattern Recognition and Machine Learning*. Springer, 2006.
- [12] D. Hernández-Lobato, J. M. Hernández-Lobato, and Pierre Dupont. Robust multi-class Gaussian process classification. In *Advances in Neural Information Processing Systems 24*.
- [13] M. Seeger. Expectation propagation for exponential families. Technical report, Department of EECS, University of California, Berkeley, 2006.
- [14] E. Snelson. *Flexible and efficient Gaussian process models for machine learning*. PhD thesis, Gatsby Computational Neuroscience Unit, University College London, 2007.
- [15] D.J. Newman A. Asuncion. UCI machine learning repository, 2007. Online available at: <http://www.ics.uci.edu/~mllearn/MLRepository.html>.
- [16] T. Heskes and O. Zoeter. Expectation propagation for approximate inference in dynamic Bayesian networks. In *Proceedings of the 18th Annual Conference on Uncertainty in Artificial Intelligence*, 2002.
- [17] A. Gelman, A. Vehtari, P. Jylänki, C. Robert, N. Chopin, and J.P. Cunningham. Expectation propagation as a way of life. *ArXiv e-prints*, 2014. arXiv:1412.4869.
- [18] Y. Qi, A.H. Abdel-Gawad, and T.P. Minka. Sparse-posterior Gaussian processes for general likelihoods. In *Proceedings of the Twenty-Sixth Conference on Uncertainty in Artificial Intelligence*, 2010.
- [19] M.D. Zeiler. ADADELTA: An adaptive learning rate method. *ArXiv e-prints*, 2012. arXiv:1212.5701.
- [20] T. Minka. *A Family of Algorithms for Approximate Bayesian Inference*. PhD thesis, MIT, 2001.
- [21] D. Hernández-Lobato. *Prediction Based on Averages over Automatically Induced Learners: Ensemble Methods and Bayesian Techniques*. PhD thesis, Universidad Autónoma de Madrid, 2009.
- [22] M. Van Gerven, B. Cseke, R. Oostenveld, and T. Heskes. Bayesian source localization with the multivariate Laplace prior. In *Advances in Neural Information Processing Systems 22*, pages 1901–1909, 2009.
- [23] K. B. Petersen and M. S. Pedersen. *The matrix cookbook*, 2012. Version 20121115.

A Supplementary Material

Here we give all the necessary details to implement the EP algorithm for the proposed method described in the main manuscript, *i.e.* SEP. In particular, we describe how to compute the EP posterior approximation from the product of all approximate factors and how to implement the EP updates to refine each approximate factor. We also give an intuitive idea about how to compute the EP approximation to the marginal likelihood and its gradients. Note that the updates described are very similar to the ones in [20].

A.1 Reconstruction of the posterior approximation

In this section we show how to obtain the posterior approximation as the normalized product of the approximate factors $\tilde{\phi}_i(\bar{\mathbf{f}})$ and the prior $p(\bar{\mathbf{f}}|\bar{\mathbf{X}})$. From the main manuscript, we know that these factors have the following form:

$$\tilde{\phi}_i(\bar{\mathbf{f}}) = \tilde{s}_i \exp \left\{ -\frac{\tilde{\nu}_i}{2} \bar{\mathbf{f}}^T \mathbf{v}_i \mathbf{v}_i^T \bar{\mathbf{f}} + \tilde{\mu}_i \bar{\mathbf{f}}^T \mathbf{v}_i \right\}, \quad (10)$$

$$p(\bar{\mathbf{f}}|\bar{\mathbf{X}}) = \mathcal{N}(\bar{\mathbf{f}}|\mathbf{0}, \mathbf{K}_{\bar{\mathbf{f}}\bar{\mathbf{f}}}), \quad (11)$$

where $\mathbf{v}_i = \mathbf{K}_{\bar{\mathbf{f}}\bar{\mathbf{f}}}^{-1} \mathbf{K}_{\bar{\mathbf{f}}f_i}$ and $\mathbf{K}_{\bar{\mathbf{f}}\bar{\mathbf{f}}}$ is a covariance matrix of size $m \times m$ with the prior covariance among the values associated to the inducing points $\bar{\mathbf{X}}$. Both the approximate factors and the prior are Gaussian, a family of distributions that is closed under product and division. The consequence is that $q(\bar{\mathbf{f}}) = \prod_{i=1}^n \tilde{\phi}_i(\bar{\mathbf{f}}) p(\bar{\mathbf{f}}|\bar{\mathbf{X}}) / Z_q$ is also Gaussian. In particular, $q(\bar{\mathbf{f}}) = \mathcal{N}(\bar{\mathbf{f}}|\boldsymbol{\mu}, \boldsymbol{\Sigma})$. To obtain the parameters of q we can use the formulas given in the Appendix of [21]. This gives,

$$\boldsymbol{\Sigma} = \left(\mathbf{K}_{\bar{\mathbf{f}}\bar{\mathbf{f}}}^{-1} + \boldsymbol{\Upsilon} \boldsymbol{\Delta} \boldsymbol{\Upsilon}^T \right)^{-1}, \quad (12)$$

$$\boldsymbol{\mu} = \boldsymbol{\Sigma} \boldsymbol{\Upsilon} \tilde{\boldsymbol{\mu}} \quad (13)$$

where $\boldsymbol{\Delta}$ is a diagonal matrix with diagonal entries equal to $\tilde{\nu}_i$, $\boldsymbol{\Upsilon}$ is a matrix whose i -th column is equal to \mathbf{v}_i , and $\tilde{\boldsymbol{\mu}}$ is a vector whose i -th component is equal to $\tilde{\mu}_i$. These computations have a cost $\mathcal{O}(nm^2)$, under the assumption that $m \ll n$. Otherwise the cost is $\mathcal{O}(m^3)$.

A.2 Computation of the cavity distribution

Before the update of each $\tilde{\phi}_i$, the first step is to compute the cavity distribution $q^{\setminus i} \propto q / \tilde{\phi}_i$. Because q and $\tilde{\phi}_i$ are Gaussians, so it is $q^{\setminus i}$. In particular, $q^{\setminus i}(\bar{\mathbf{f}}) = \mathcal{N}(\bar{\mathbf{f}}|\boldsymbol{\mu}^{\setminus i}, \boldsymbol{\Sigma}^{\setminus i})$. The parameters of $q^{\setminus i}$ can also be obtained using the formulas given in the Appendix of [21]. That is,

$$\boldsymbol{\Sigma}^{\setminus i} = \left(\boldsymbol{\Sigma}^{-1} - \tilde{\nu}_i \mathbf{v}_i \mathbf{v}_i^T \right)^{-1} = \boldsymbol{\Sigma} + (\tilde{\nu}_i^{-1} - \mathbf{v}_i^T \boldsymbol{\Sigma} \mathbf{v}_i)^{-1} \boldsymbol{\Sigma} \mathbf{v}_i \mathbf{v}_i^T \boldsymbol{\Sigma}, \quad (14)$$

$$\boldsymbol{\mu}^{\setminus i} = \boldsymbol{\Sigma}^{\setminus i} \left(\boldsymbol{\Sigma}^{-1} \boldsymbol{\mu} - \tilde{\mu}_i \mathbf{v}_i \right) = \boldsymbol{\mu} + \boldsymbol{\Sigma}^{\setminus i} \mathbf{v}_i \left(\tilde{\nu}_i \mathbf{v}_i^T \boldsymbol{\mu} - \tilde{\mu}_i \right), \quad (15)$$

where we have used the Woodbury matrix identity and that $\boldsymbol{\Sigma}^{-1} = (\boldsymbol{\Sigma}^{\setminus i})^{-1} + \tilde{\nu}_i \mathbf{v}_i \mathbf{v}_i^T$. These computations have a cost that is $\mathcal{O}(m^2)$.

A.3 Update of the approximate factors

In this section we show how to find the approximate factors $\tilde{\phi}_i$. For that we consider that the corresponding cavity distribution $q^{\setminus i}$ has already been computed. From the main manuscript, we know that the exact factor to be approximated is:

$$\phi_i(\bar{\mathbf{f}}) = \int \Phi(y_i f_i) \mathcal{N}(f_i | m_i, s_i) df_i = \Phi \left(\frac{y_i m_i}{\sqrt{s_i + 1}} \right), \quad (16)$$

where $\Phi(\cdot)$ is the c.d.f. of a standard Gaussian, $m_i = \mathbf{K}_{f_i \bar{\mathbf{f}}} \mathbf{K}_{\bar{\mathbf{f}}\bar{\mathbf{f}}}^{-1} \bar{\mathbf{f}}$ and $s_i = \mathbf{K}_{f_i f_i} - \mathbf{K}_{f_i \bar{\mathbf{f}}} \mathbf{K}_{\bar{\mathbf{f}}\bar{\mathbf{f}}}^{-1} \mathbf{K}_{\bar{\mathbf{f}} f_i}$. We compute Z_i , *i.e.*, the normalization constant of $\phi_i q^{\setminus i}$, as follows:

$$Z_i = \int \Phi \left(\frac{y_i m_i}{\sqrt{s_i + 1}} \right) \mathcal{N}(\bar{\mathbf{f}} | \boldsymbol{\mu}^{\setminus i}, \boldsymbol{\Sigma}^{\setminus i}) d\bar{\mathbf{f}} = \Phi \left(\frac{y_i a_i}{\sqrt{b_i}} \right), \quad (17)$$

where $a_i = \mathbf{K}_{f_i \bar{\mathbf{f}}} \mathbf{K}_{\bar{\mathbf{f}}\bar{\mathbf{f}}}^{-1} \boldsymbol{\mu}^{\setminus i}$ and $b_i = 1 + \mathbf{K}_{f_i f_i} - \mathbf{K}_{f_i \bar{\mathbf{f}}} \mathbf{K}_{\bar{\mathbf{f}}\bar{\mathbf{f}}}^{-1} \mathbf{K}_{\bar{\mathbf{f}} f_i} + \mathbf{K}_{f_i \bar{\mathbf{f}}} \mathbf{K}_{\bar{\mathbf{f}}\bar{\mathbf{f}}}^{-1} \boldsymbol{\Sigma}^{\setminus i} \mathbf{K}_{\bar{\mathbf{f}}\bar{\mathbf{f}}}^{-1} \mathbf{K}_{\bar{\mathbf{f}} f_i}$. By using the equations given in the Appendix of [21] it is possible to obtain the moments, *i.e.*, the mean $\hat{\boldsymbol{\mu}}$ and the

covariances $\hat{\Sigma}$ of $\phi_i q^{\setminus i}$, from the derivatives of $\log Z_i$ with respect to the parameters of $q^{\setminus i}$. Namely,

$$\hat{\mathbf{m}} = \boldsymbol{\mu}^{\setminus i} + \boldsymbol{\Sigma}^{\setminus i} \frac{\partial \log Z_i}{\partial \boldsymbol{\mu}^{\setminus i}} = \boldsymbol{\mu}^{\setminus i} + \alpha_i \boldsymbol{\Sigma}^{\setminus i} \mathbf{K}_{\mathbf{f}\mathbf{f}}^{-1} \mathbf{K}_{\mathbf{f}f_i}, \quad (18)$$

$$\begin{aligned} \hat{\Sigma} &= \boldsymbol{\Sigma}^{\setminus i} - \boldsymbol{\Sigma}^{\setminus i} \left(\left(\frac{\partial \log Z_i}{\partial \boldsymbol{\mu}^{\setminus i}} \right) \left(\frac{\partial \log Z_i}{\partial \boldsymbol{\mu}^{\setminus i}} \right)^{\text{T}} - 2 \frac{\partial \log Z_i}{\partial \boldsymbol{\Sigma}^{\setminus i}} \right) \boldsymbol{\Sigma}^{\setminus i} \\ &= \boldsymbol{\Sigma}^{\setminus i} - \boldsymbol{\Sigma}^{\setminus i} \mathbf{K}_{\mathbf{f}\mathbf{f}}^{-1} \mathbf{K}_{\mathbf{f}f_i} \mathbf{K}_{f_i\mathbf{f}} \mathbf{K}_{\mathbf{f}\mathbf{f}}^{-1} \boldsymbol{\Sigma}^{\setminus i} \left(\alpha_i^2 + \frac{\alpha_i a_i}{b_i} \right), \end{aligned} \quad (19)$$

where

$$\alpha_i = \frac{\mathcal{N}(y_i a_i / \sqrt{b_i} | 0, 1) y_i}{\Phi(y_i a_i / \sqrt{b_i}) b_i}. \quad (20)$$

These are very similar to the EP updates described in [20].

Given the previous updates, it is possible to find the parameters of the corresponding approximate factor $\tilde{\phi}_i$, which is simply obtained as $\tilde{\phi}_i = Z_i q^{\text{new}} / q^{\setminus i}$, where q^{new} is a Gaussian distribution with the mean and the covariances of $\phi_i q^{\setminus i}$. We show here that the precision matrix of the approximate factor $\tilde{\phi}_i$ has a low rank form. Denote with $\tilde{\mathbf{V}}_i$ to such matrix. Let also $\tilde{\mathbf{m}}_i$ be the precision matrix of $\tilde{\phi}_i$ times the mean vector. Define $\mathbf{v}_i = \mathbf{K}_{\mathbf{f}\mathbf{f}}^{-1} \mathbf{K}_{\mathbf{f}f_i}$. Then, by using the equations given in the Appendix of [21] we have that

$$\tilde{\mathbf{V}}_i = \hat{\Sigma}^{-1} - \left(\boldsymbol{\Sigma}^{\setminus i} \right)^{-1} = \left(\boldsymbol{\Sigma}^{\setminus i} \right)^{-1} + \mathbf{v}_i \mathbf{v}_i^{\text{T}} \tilde{\nu}_i - \left(\boldsymbol{\Sigma}^{\setminus i} \right)^{-1} = \mathbf{v}_i \mathbf{v}_i^{\text{T}} \tilde{\nu}_i \quad (21)$$

$$\tilde{\mathbf{m}}_i = \hat{\Sigma}^{-1} \hat{\mathbf{m}} - \left(\boldsymbol{\Sigma}^{\setminus i} \right)^{-1} \boldsymbol{\mu}^{\setminus i} = \left(\alpha_i + a_i \tilde{\nu}_i + \alpha_i \mathbf{v}_i^{\text{T}} \boldsymbol{\Sigma}^{\setminus i} \mathbf{v}_i \tilde{\nu}_i \right) \mathbf{v}_i = \tilde{\mu}_i \mathbf{v}_i \quad (22)$$

where we have used the Woodbury matrix identity, the definition of $\hat{\mathbf{m}}$ and $\hat{\Sigma}$, and

$$\tilde{\nu}_i = \left[\left(\alpha_i^2 + \frac{\alpha_i a_i}{b_i} \right)^{-1} + \mathbf{v}_i^{\text{T}} \boldsymbol{\Sigma}^{\setminus i} \mathbf{v}_i \right]^{-1} \quad \tilde{\mu}_i = \alpha_i + a_i \tilde{\nu}_i + \alpha_i \mathbf{v}_i^{\text{T}} \boldsymbol{\Sigma}^{\setminus i} \mathbf{v}_i \tilde{\nu}_i. \quad (23)$$

Thus, we see that the approximate factor has the form described in (10).

Once we have the parameters of the approximate factor $\tilde{\phi}_i$, we can compute the value of \tilde{s}_i in (10) which guarantees that the approximate factor integrates the same as the exact factor with respect to $q^{\setminus i}$. Let $\boldsymbol{\theta}$ be the natural parameters of q after the update. Similarly, let $\boldsymbol{\theta}^{\setminus i}$ be the natural parameters of $q^{\setminus i}$. Then,

$$\tilde{s}_i = \log Z_i + g(\boldsymbol{\theta}^{\setminus i}) - g(\boldsymbol{\theta}), \quad (24)$$

where $g(\boldsymbol{\theta})$ is the log-normalizer of a multi-variate Gaussian with natural parameters $\boldsymbol{\theta}$.

A.4 Parallel EP updates and damping

The updates described for the approximate factors are done in parallel. That is, we compute the required quantities to update each factor $\tilde{\phi}_i$ at the same time using (23). Then, the new parameters of each approximate factor $\tilde{\nu}_i$ and $\tilde{\mu}_i$ are computed based on the previous ones. Finally, after the parallel update, we recompute q as indicated in Section A.1. All these operations have a closed-form and involve only matrix multiplications with cost $\mathcal{O}(nm^2)$, where n is the number of samples and m is the number of inducing points.

Parallel EP updates were first proposed in [22] and have been also used in the context of Gaussian process classification in [12]. Parallel EP updates are much faster than sequential updates because they avoid having to code loops over the training instances. All operations simply involve matrix multiplications which are significantly faster as a consequence of using the BLAS library (available in most scientific programming languages such as R, matlab or Python) that has been significantly optimized.

Parallel updates may deteriorate EP convergence in some situations. Thus, we also use damped EP updates. Damping is a standard approach in EP algorithms which significantly improves convergence. The

idea is to avoid large changes in the parameters $\tilde{\nu}_i$ and $\tilde{\mu}_i$ of the approximate factors $\tilde{\phi}_i$. For this, the parameters after the EP updates are set to be a linear combination of the old and the new parameters. In particular,

$$\tilde{\nu}_i = \rho \tilde{\nu}_i^{\text{new}} + (1 - \rho) \tilde{\nu}_i^{\text{old}}, \quad \tilde{\mu}_i = \rho \tilde{\mu}_i^{\text{new}} + (1 - \rho) \tilde{\mu}_i^{\text{old}}, \quad (25)$$

where $\rho \in [0, 1]$ is a parameter controlling the amount of damping. If $\rho = 1$ there is no damping and if $\rho = 0$ the parameters of each $\tilde{\phi}_i$ are not updated at all. In our experiments we set $\rho = 0.5$ when doing batch training and we set $\rho = 0.99$ when the training process is done in a stochastic fashion using minibatches (in this case we do more frequent reconstructions of q , *i.e.*, after processing each minibatch and less damping is needed). Damping does not change the fixed points of EP.

A.5 Estimate of the marginal likelihood

As indicated in the main manuscript, the estimate of the marginal likelihood is given by

$$\log Z_q = g(\boldsymbol{\theta}) - g(\boldsymbol{\theta}_{\text{prior}}) + \sum_{i=1}^n \log \tilde{Z}_i \quad \log \tilde{Z}_i = \log Z_i + g(\boldsymbol{\theta}^{\setminus i}) - g(\boldsymbol{\theta}), \quad (26)$$

where $\boldsymbol{\theta}$, $\boldsymbol{\theta}^{\setminus i}$ and $\boldsymbol{\theta}_{\text{prior}}$ are the natural parameters of q , $q^{\setminus i}$ and $p(\bar{\mathbf{f}}|\bar{\mathbf{X}})$, respectively; and $g(\boldsymbol{\theta})$ is the log-normalizer of a multivariate Gaussian distribution with natural parameters $\boldsymbol{\theta}$. Let \mathbf{m} and \mathbf{S} be the variance and the mean, respectively, of a Gaussian distribution over m dimensions with natural parameters $\boldsymbol{\theta}'$. Then,

$$g(\boldsymbol{\theta}') = \frac{m}{2} \log 2\pi + \frac{1}{2} \log |\mathbf{S}| + \frac{1}{2} \mathbf{m}^T \mathbf{S}^{-1} \mathbf{m}. \quad (27)$$

The consequence is that

$$\log Z_q = \frac{1}{2} \log |\boldsymbol{\Sigma}| + \frac{1}{2} \boldsymbol{\mu}^T \boldsymbol{\Sigma}^{-1} \boldsymbol{\mu} - \frac{1}{2} \log |\mathbf{K}_{\text{ff}}| + \sum_{i=1}^n \log \tilde{Z}_i, \quad (28)$$

with

$$\begin{aligned} \tilde{Z}_i &= \log Z_i + \frac{1}{2} \log |\boldsymbol{\Sigma}^{\setminus i}| + \frac{1}{2} (\boldsymbol{\mu}^{\setminus i})^T (\boldsymbol{\Sigma}^{\setminus i})^{-1} \boldsymbol{\mu}^{\setminus i} - \frac{1}{2} \log |\boldsymbol{\Sigma}| - \frac{1}{2} \boldsymbol{\mu}^T \boldsymbol{\Sigma}^{-1} \boldsymbol{\mu} \\ &= \log Z_i - 2\tilde{\mu}_i \mathbf{v}_i^T \boldsymbol{\mu} + \tilde{\mu}_i^2 \mathbf{v}_i^T \boldsymbol{\Sigma} \mathbf{v}_i + (\boldsymbol{\mu}^T \mathbf{v}_i)^2 C_i - 2\boldsymbol{\mu}^T \mathbf{v}_i \mathbf{v}_i^T \boldsymbol{\Sigma} \mathbf{v}_i \tilde{\mu}_i C_i \\ &\quad + \tilde{\mu}_i^2 C_i (\mathbf{v}_i^T \boldsymbol{\Sigma} \mathbf{v}_i)^2 + \frac{1}{2} \log(1 - \tilde{\nu}_i \mathbf{v}_i \boldsymbol{\Sigma} \mathbf{v}_i), \end{aligned} \quad (29)$$

where we have used that $(\boldsymbol{\Sigma}^{\setminus i})^{-1} = \boldsymbol{\Sigma}^{-1} - \tilde{\nu}_i \mathbf{v}_i \mathbf{v}_i^T$, the Woodbury matrix identity, the matrix determinant lemma, that $\boldsymbol{\mu}^{\setminus i} = \boldsymbol{\Sigma}^{\setminus i} (\boldsymbol{\Sigma}^{-1} \boldsymbol{\mu} - \tilde{\mu}_i \mathbf{v}_i)$, and set $C_i = (\tilde{\nu}_i^{-1} - \mathbf{v}_i \boldsymbol{\Sigma} \mathbf{v}_i)^{-1}$. The consequence is that the computation of $\log Z_q$ can be done with cost $\mathcal{O}(nm^2)$ if $m \ll n$.

A.6 Gradient of $\log Z_q$ after convergence

In this section we show that the gradient of $\log Z_q$, after convergence, is given by the expression given in the main manuscript. For that, we extend the results of [13]. Denote by ξ_j to one hyper-parameter of the model. That is, a parameter of the covariance function k or a component of the inducing points. Then, the gradient of $\log Z_q$ with respect to this parameter is:

$$\begin{aligned} \frac{\partial \log Z_q}{\partial \xi_j} &= \left(\frac{\partial g(\boldsymbol{\theta})}{\partial \boldsymbol{\theta}} \right)^T \frac{\partial \boldsymbol{\theta}}{\partial \xi_j} - \left(\frac{\partial g(\boldsymbol{\theta}_{\text{prior}})}{\partial \boldsymbol{\theta}_{\text{prior}}} \right)^T \frac{\partial \boldsymbol{\theta}_{\text{prior}}}{\partial \xi_j} + \sum_{i=1}^n \frac{\partial \log Z_i}{\partial \xi_j} \\ &\quad + \sum_{i=1}^n \left(\frac{\partial g(\boldsymbol{\theta}^{\setminus i})}{\partial \boldsymbol{\theta}^{\setminus i}} \right)^T \frac{\partial \boldsymbol{\theta}^{\setminus i}}{\partial \xi_j} - \sum_{i=1}^n \left(\frac{\partial g(\boldsymbol{\theta})}{\partial \boldsymbol{\theta}} \right)^T \frac{\partial \boldsymbol{\theta}}{\partial \xi_j}, \end{aligned} \quad (30)$$

where $\boldsymbol{\theta}$, $\boldsymbol{\theta}^{\setminus i}$ and $\boldsymbol{\theta}_{\text{prior}}$ are the natural parameters of q , $q^{\setminus i}$, and the prior $p(\bar{\mathbf{f}}|\bar{\mathbf{X}})$, respectively. Importantly, the term $\log Z_i$ depends on ξ_j in a direct way, *i.e.*, because the exact likelihood factor $\phi_i(\bar{\mathbf{f}}) = \int \Phi(y_i f_i) \mathcal{N}(f_i | m_i, s_i) df_i = \Phi(y_i m_i / \sqrt{s_i + 1})$, with $m_i = \mathbf{K}_{f_i \bar{\mathbf{f}}} \mathbf{K}_{\bar{\mathbf{f}} \bar{\mathbf{f}}}^{-1} \bar{\mathbf{f}}$ and $s_i = \mathbf{K}_{f_i f_i} - \mathbf{K}_{f_i \bar{\mathbf{f}}} \mathbf{K}_{\bar{\mathbf{f}} \bar{\mathbf{f}}}^{-1} \mathbf{K}_{\bar{\mathbf{f}} f_i}$, depends on ξ_j , and in an indirect way, *i.e.*, because the natural parameters of the cavity distribution $q^{\setminus i}$, $\boldsymbol{\theta}^{\setminus i}$, depend on ξ_j . In particular,

$$Z_i = \int \phi_i(\bar{\mathbf{f}}) \exp \left\{ \left(\boldsymbol{\theta}^{\setminus i} \right)^{\text{T}} h(\bar{\mathbf{f}}) - g(\boldsymbol{\theta}^{\setminus i}) \right\} d\bar{\mathbf{f}}, \quad (31)$$

where $h(\bar{\mathbf{f}})$ are the sufficient statistics of $q^{\setminus i}$. The consequence is that

$$\begin{aligned} \frac{\partial \log Z_i}{\partial \xi_j} &= \overbrace{\frac{\partial \log Z_i}{\partial \xi}}^{\text{Only } \phi_i(\bar{\mathbf{f}}) \text{ changes}} + \left(\frac{\partial \log Z_i}{\partial \boldsymbol{\theta}^{\setminus i}} \right)^{\text{T}} \frac{\partial \boldsymbol{\theta}^{\setminus i}}{\partial \xi_j} \\ &= \overbrace{\frac{\partial \log Z_i}{\partial \xi_j}}^{\text{Only } \phi_i(\bar{\mathbf{f}}) \text{ changes}} + \boldsymbol{\eta}^{\text{T}} \frac{\partial \boldsymbol{\theta}^{\setminus i}}{\partial \xi_j} - \left(\boldsymbol{\eta}^{\setminus i} \right)^{\text{T}} \frac{\partial \boldsymbol{\theta}^{\setminus i}}{\partial \xi_j}, \end{aligned} \quad (32)$$

where $\boldsymbol{\eta}$ and $\boldsymbol{\eta}^{\setminus i}$ are the expected sufficient statistics under the posterior approximation q and the cavity distribution $q^{\setminus i}$. Recall that we have assumed convergence which leads to a match of the moments between $Z_i^{-1} \phi_i q^{\setminus i}$ and q .

If we substitute (32) in (30) we have that:

$$\begin{aligned} \frac{\partial \log Z_i}{\partial \xi_j} &= \left(\frac{\partial g(\boldsymbol{\theta})}{\partial \boldsymbol{\theta}} \right)^{\text{T}} \frac{\partial \boldsymbol{\theta}}{\partial \xi_j} - \left(\frac{\partial g(\boldsymbol{\theta}_{\text{prior}})}{\partial \boldsymbol{\theta}_{\text{prior}}} \right)^{\text{T}} \frac{\partial \boldsymbol{\theta}_{\text{prior}}}{\partial \xi_j} + \sum_{i=1}^n \frac{\partial \log Z_i}{\partial \xi_j} + \sum_{i=1}^n \boldsymbol{\eta}^{\text{T}} \frac{\partial \boldsymbol{\theta}^{\setminus i}}{\partial \xi_j} \\ &\quad - \sum_{i=1}^n \left(\boldsymbol{\eta}^{\setminus i} \right)^{\text{T}} \frac{\partial \boldsymbol{\theta}^{\setminus i}}{\partial \xi_j} + \sum_{i=1}^n \left(\frac{\partial g(\boldsymbol{\theta}^{\setminus i})}{\partial \boldsymbol{\theta}^{\setminus i}} \right)^{\text{T}} \frac{\partial \boldsymbol{\theta}^{\setminus i}}{\partial \xi_j} - \sum_{i=1}^n \left(\frac{\partial g(\boldsymbol{\theta})}{\partial \boldsymbol{\theta}} \right)^{\text{T}} \frac{\partial \boldsymbol{\theta}}{\partial \xi_j} \\ &= \boldsymbol{\eta}^{\text{T}} \frac{\partial \boldsymbol{\theta}}{\partial \xi_j} - \left(\boldsymbol{\eta}_{\text{prior}} \right)^{\text{T}} \frac{\partial \boldsymbol{\theta}_{\text{prior}}}{\partial \xi_j} + \sum_{i=1}^n \frac{\partial \log Z_i}{\partial \xi_j} + \sum_{i=1}^n \boldsymbol{\eta}^{\text{T}} \frac{\partial \boldsymbol{\theta}^{\setminus i}}{\partial \xi_j} \\ &\quad - \sum_{i=1}^n \boldsymbol{\eta}^{\setminus i} \frac{\partial \boldsymbol{\theta}^{\setminus i}}{\partial \xi_j} + \sum_{i=1}^n \left(\boldsymbol{\eta}^{\setminus i} \right)^{\text{T}} \frac{\partial \boldsymbol{\theta}^{\setminus i}}{\partial \xi_j} - \sum_{i=1}^n \boldsymbol{\eta}^{\text{T}} \frac{\partial \boldsymbol{\theta}}{\partial \xi_j} \\ &= \boldsymbol{\eta}^{\text{T}} \frac{\partial \boldsymbol{\theta}}{\partial \xi_j} - \left(\boldsymbol{\eta}_{\text{prior}} \right)^{\text{T}} \frac{\partial \boldsymbol{\theta}_{\text{prior}}}{\partial \xi_j} + \sum_{i=1}^n \frac{\partial \log Z_i}{\partial \xi_j} + \sum_{i=1}^n \boldsymbol{\eta}^{\text{T}} \left(\frac{\partial \boldsymbol{\theta}^{\setminus i}}{\partial \xi_j} - \frac{\partial \boldsymbol{\theta}}{\partial \xi_j} \right) \\ &= \boldsymbol{\eta}^{\text{T}} \frac{\partial \boldsymbol{\theta}}{\partial \xi_j} - \left(\boldsymbol{\eta}_{\text{prior}} \right)^{\text{T}} \frac{\partial \boldsymbol{\theta}_{\text{prior}}}{\partial \xi_j} + \sum_{i=1}^n \frac{\partial \log Z_i}{\partial \xi_j} - \sum_{i=1}^n \boldsymbol{\eta}^{\text{T}} \frac{\partial \boldsymbol{\theta}_i}{\partial \xi_j} \\ &= \boldsymbol{\eta}^{\text{T}} \frac{\partial \boldsymbol{\theta}}{\partial \xi_j} - \left(\boldsymbol{\eta}_{\text{prior}} \right)^{\text{T}} \frac{\partial \boldsymbol{\theta}_{\text{prior}}}{\partial \xi_j} + \sum_{i=1}^n \frac{\partial \log Z_i}{\partial \xi_j} - \boldsymbol{\eta}^{\text{T}} \frac{\partial \boldsymbol{\theta}^{\setminus \text{prior}}}{\partial \xi_j} \\ &= \boldsymbol{\eta}^{\text{T}} \left(\frac{\partial \boldsymbol{\theta}}{\partial \xi_j} - \frac{\partial \boldsymbol{\theta}^{\setminus \text{prior}}}{\partial \xi_j} \right) - \left(\boldsymbol{\eta}_{\text{prior}} \right)^{\text{T}} \frac{\partial \boldsymbol{\theta}_{\text{prior}}}{\partial \xi_j} + \sum_{i=1}^n \frac{\partial \log Z_i}{\partial \xi_j} \\ &= \boldsymbol{\eta}^{\text{T}} \frac{\partial \boldsymbol{\theta}_{\text{prior}}}{\partial \xi_j} - \left(\boldsymbol{\eta}_{\text{prior}} \right)^{\text{T}} \frac{\partial \boldsymbol{\theta}_{\text{prior}}}{\partial \xi_j} + \sum_{i=1}^n \frac{\partial \log Z_i}{\partial \xi_j}, \end{aligned} \quad (33)$$

where $\boldsymbol{\eta}_{\text{prior}}$ are the expected sufficient statistics of the prior and we have used that $\boldsymbol{\theta} = \boldsymbol{\theta}_{\text{prior}} + \sum_{i=1}^n \boldsymbol{\theta}_i$, with $\boldsymbol{\theta}_i$ the natural parameters of the approximate factor $\tilde{\phi}_i$, and that $\boldsymbol{\theta}^{\setminus \text{prior}} = \sum_{i=1}^n \boldsymbol{\theta}_i$. Thus, at convergence the approximate factors can be considered to be fixed. In particular, (33) is the gradient obtained under the assumption that all $\tilde{\phi}_i$ remain fixed and do not change with the model hyper-parameters.

The chain rule of derivatives has to be taken with care in the previous expression. Since the natural parameters and the expected sufficient statistics are often expressed in the form of matrices, the chain rule for matrix derivatives has to be employed in practice (see [23, Sec. 2.8.1]). The consequence is that

$$\boldsymbol{\eta}^\top \frac{\partial \boldsymbol{\theta}_{\text{prior}}}{\partial \xi_j} - (\boldsymbol{\eta}_{\text{prior}})^\top \frac{\partial \boldsymbol{\theta}_{\text{prior}}}{\partial \xi_j} = -0.5 \text{tr} \left(\mathbf{M}^\top \frac{\mathbf{K}_{\bar{\mathbf{f}}\bar{\mathbf{f}}}}{\partial \xi_j} \right), \quad (34)$$

where

$$\mathbf{M} = \mathbf{K}_{\bar{\mathbf{f}}\bar{\mathbf{f}}}^{-1} - \mathbf{K}_{\bar{\mathbf{f}}\bar{\mathbf{f}}}^{-1} \boldsymbol{\Sigma} \mathbf{K}_{\bar{\mathbf{f}}\bar{\mathbf{f}}}^{-1} - \mathbf{K}_{\bar{\mathbf{f}}\bar{\mathbf{f}}}^{-1} \boldsymbol{\mu} \boldsymbol{\mu}^\top \mathbf{K}_{\bar{\mathbf{f}}\bar{\mathbf{f}}}^{-1}. \quad (35)$$

In the case of computing the derivatives with respect to the inducing points several contractions occur, as indicated in [14]. The computational cost of obtaining these derivatives is $\mathcal{O}(m^3)$.

The derivatives with respect to each $\log Z_i$ can be computed also efficiently using the chain rule for matrix derivatives indicated in [23, Sec. 2.8.1]. The computational cost of obtaining these derivatives is $\mathcal{O}(nm^2)$. Furthermore, several standard properties of the trace can be employed to simplify the computations. In particular, the trace is invariant to cyclic rotations. Namely, $\text{tr}(\mathbf{ABCD}) = \text{tr}(\mathbf{DABC})$.

By using the gradients described, it is possible to maximize $\log Z_q$ to find good values for the model hyper-parameters. However, as stated in the main manuscript, we do not wait until EP converges for doing the update. In particular, we perform an update of the hyper-parameters considering the $\tilde{\phi}_i$ as fixed, after each parallel refinement of the approximate factors. Because we are updating the approximate factors too, we cannot simply expect that such steps always improve on the objective $\log Z_q$, but in practice they seem to work very well. In our experiments we use an adaptive learning rate that is different for each hyper-parameter. In particular, we increase the learning rate by 2% if the sign of the estimate of the gradient for that hyper-parameter does not change between two consecutive iterations. If a change is observed, we reduce we multiply the learning rate by 1/2. If a stochastic approximation of the estimate of the gradient is employed, we use the ADADELTA method to estimate the learning rate [19].

A.7 Predictive distribution

Once the training process is complete, we can use the posterior approximation q for making predictions about the class label $y_\star \in \{-1, 1\}$ of a new instance \mathbf{x}_\star . In that case, we compute first an approximate posterior for the Gaussian process evaluated at the target location, *i.e.*, $f(\mathbf{x}_\star)$, which is summarized as f_\star :

$$\begin{aligned} p(f_\star | \mathbf{y}, \bar{\mathbf{X}}) &\approx \int p(f_\star | \bar{\mathbf{f}}) q(\bar{\mathbf{f}}) d\bar{\mathbf{f}} \\ &\approx \int \mathcal{N}(f_\star | \mathbf{K}_{f_\star \bar{\mathbf{f}}} \mathbf{K}_{\bar{\mathbf{f}}\bar{\mathbf{f}}}^{-1} \bar{\mathbf{f}}, \mathbf{K}_{f_\star f_\star} - \mathbf{K}_{f_\star \bar{\mathbf{f}}} \mathbf{K}_{\bar{\mathbf{f}}\bar{\mathbf{f}}}^{-1} \mathbf{K}_{\bar{\mathbf{f}} f_\star}) \mathcal{N}(\bar{\mathbf{f}} | \boldsymbol{\mu}, \boldsymbol{\Sigma}) d\bar{\mathbf{f}} \\ &\approx \mathcal{N}(f_\star | m_\star, s_\star), \end{aligned} \quad (36)$$

where $m_\star = \mathbf{K}_{f_\star \bar{\mathbf{f}}} \mathbf{K}_{\bar{\mathbf{f}}\bar{\mathbf{f}}}^{-1} \boldsymbol{\mu}$ and $s_\star = \mathbf{K}_{f_\star f_\star} - \mathbf{K}_{f_\star \bar{\mathbf{f}}} \mathbf{K}_{\bar{\mathbf{f}}\bar{\mathbf{f}}}^{-1} \mathbf{K}_{\bar{\mathbf{f}} f_\star} + \mathbf{K}_{f_\star \bar{\mathbf{f}}} \mathbf{K}_{\bar{\mathbf{f}}\bar{\mathbf{f}}}^{-1} \boldsymbol{\Sigma} \mathbf{K}_{\bar{\mathbf{f}}\bar{\mathbf{f}}}^{-1} \mathbf{K}_{\bar{\mathbf{f}} f_\star}$. $\mathbf{K}_{f_\star f_\star}$ and $\mathbf{K}_{f_\star \bar{\mathbf{f}}}$ contain the prior variance of f_\star and the prior covariances between f_\star and $\bar{\mathbf{f}}$, respectively. The approximate predictive distribution for the class label y_\star is simply:

$$p(y_\star | \mathbf{y}, \bar{\mathbf{X}}) = \int p(y_\star | f_\star) p(f_\star | \mathbf{y}, \bar{\mathbf{X}}) df_\star = \int \Phi(y_\star f_\star) \mathcal{N}(f_\star | m_\star, s_\star) df_\star = \Phi \left(\frac{y_\star m_\star}{\sqrt{s_\star + 1}} \right), \quad (37)$$

where $\Phi(\cdot)$ is the c.d.f of a standard Gaussian distribution.